

Adsorption Behavior, Electronical and Thermodynamic Properties of Ornidazole Drug on C₆₀ Fullerene Doped with Si, B and Al: A Quantum Mechanical Simulation

M.H. Fekri*, R. Bazvand, M. Solymani and M. Razavi Mehr

Department of Chemistry, Ayatollah Borujerdi University, Borujerd, Iran

(Received 17 August 2020, Accepted 4 December 2020)

In this research, we investigated the interaction behavior of ornidazole drug on the surface of pristine as well as doped C₆₀ fullerene with Si, B and Al using density functional theory (DFT) at the B3LYP/6-31G* level in gas phase and water. To study the ornidazole adsorption properties on C₆₀, we replaced a carbon atom with B, Si and Al atoms. After optimization of the structures, various parameters such as HOMO and LUMO energies, gap energy, adsorption energy, chemical hardness, chemical potential, dipole moment, electrophilicity index and thermodynamics data were calculated. The binding energy of ornidazole to the doped fullerenes is much more negative than that for the pristine C₆₀ and the HOMO-LUMO gaps are significantly enlarged. Our results show that doping may improve C₆₀ drug delivery properties.

Keywords: Ornidazole, Density functional theory (DFT), Fullerene C₆₀, Chemical potential, Doping

INTRODUCTION

Ornidazole (Orn.) is a nitroimidazole antibiotic which is similar to metronidazole. Oral administration ornidazole is rapidly absorbed. It is an effective treatment for amoebas and unicellular such as Giardia, Entamoeba, Trichomonas, and gram positive and negative anaerobic bacteria. In addition, it is used for the clostridium treatment instead of vancomycin as well as treatment of the helicobacter pylori and abdominal infections [1].

Molecular interactions of drugs are important in various processes of pharmacy, drug design, imaging, etc. Therefore, drug interactions with nanomaterials have been extensively investigated [2-5]. Among the nanostructures, fullerenes are known as suitable candidates for drug delivery in terms of suitable properties such as hydrophobic properties, unique spherical structure, efficient drug loading, ability to slowly release the drug in a controlled manner, protection of the drug's molecular structure and fewer side

effects. Due to the small size of these nanostructures, they can pass from the membranes easily and insert to the cell [6, 7]. For a nano carrier to be effective in delivering drugs to a diseased tissue, it should be able to efficiently interact with the capillary wall and “migrate” to the target tissue (e.g., tumors) before being cleared away by the reticuloendothelial system or being filtered by the lungs, liver, and spleen. It has been reported that microparticles larger than 5 μm are trapped in the capillary beds of the liver, whereas microparticles of ~1-5 μm localize within the liver where they are phagocytosed by Kupffer cells. Nanoparticles that are less than 1 μm and larger than 200 nm are easily filtered out in the spleen, while those smaller than 100 nm remain in blood vessels within fenestrae of the endothelial lining [8].

The geometry of nanocarriers (e.g., shape, aspect ratio, and ratio of particle dimensions to vessel diameter) directly affects their margination dynamics; i.e., the lateral drift of particles towards the blood vessel wall [9]. Using molecular modeling, Ferrari *et al.* showed that size can significantly affect how particles interact with tumor capillaries during

*Corresponding author. E-mail: m.h.fekri@abru.ac.ir

transport. Recent reports also suggest a significant role for particle shape in the *in vivo* performance of delivery vehicles. Specifically, shape and shape-related factors like aspect ratio or edge geometry affect the particle transport characteristics, influence cell-particle interactions, and alter drug release kinetics.

The results summarized above, demonstrate that particle aspect ratio, shape, and volume all affect cellular internalization of nanoparticles. A more comprehensive evaluation of uptake as a function of each of these particle characteristics needs to be performed. It is critical that these experiments are conducted while attempting to hold other particle properties (*i.e.*, volume, surface area, material composition) constant. Nevertheless, the theoretical modeling and *in vitro* studies taken together provide significant evidence to support the idea that nanoparticle-based drug delivery to target cells can be “controlled” through rational design of particle geometry [10].

Among nanomaterials, fullerenes have received much attention as appropriate carbon-based nanomaterials for drug delivery because of their suitable properties such as unique spherical structure, hydrophobic characteristic, versatile chemical, physical and biological properties, unique biological activities such as antioxidant capacity, efficient drug loading and fewer side effects in biological media.

In recent years, the use of computational chemistry to study drug delivery systems has increased. In fact, development of drug delivery systems needs to be studied in more details [11-13]. Fullerenes have been less studied by computational chemistry methods compared to the other nano structures. In 2017, khodam hazrati *et al.* reported a DFT method for study of B₂₄N₂₄ fullerene as a carrier for 5-fluorouracil anti-cancer drug and another study in 2020 by Bagheri Novir *et al.* used fullerene C₆₀ as drug delivery system for chloroquine drug [14,15]. Doping of the nanostructures with different functional groups is one of the common methods to increase its specific surface area. For example, Geng *et al.* [16] and Khodadadi *et al.* utilized nitrogen-doped graphene quantum dots as a drug delivery system. Their results showed that the quantum dots of graphene doped with nitrogen improve the drug performance [16,17].

In this work, Gauss View software was used to design

Orn., pristine C₆₀, and doped with Si-, B and Al and their complexes. The energies of the highest occupied and the lowest unoccupied molecular orbitals (HOMO & LUMO), gap energy (E_g) and general characteristics such as chemical potential (μ), chemical hardness (η), maximum charge transfer (ΔN_{max}), electrophilicity index (ω), *etc.* were calculated [18-23].

COMPUTATIONAL DETAILS

The purpose of this work is to investigate the interactions between Orn. drug (Fig. 1) with pristine C₆₀ and Si-, B- and Al-doped C₆₀. To appraise the most stable structure of Orn., C₆₀ and its energy, the optimization of the different configurations of the drug and C₆₀ fullerene in gas phase were carried out using B3LYP functional and 6-31G* basis set, implemented in Gaussian 09 program [24].

Adsorption energy (E_{ads.}) of Orn.-nanocarriers was calculated using the following equation:

$$E_{ads.} = [E_{Complex}] - [E_{cage.} + E_{Orn.}] \quad (1)$$

where E_{Orn.}, E_{complex} and E_{cage} are the energies of Orn., fullerene-drug complexes, and pristine fullerene doped with silicone, boron, and aluminum, respectively.

Also, cohesive energy (E_{coh}) of Orn.-nanocarriers was calculated (Table 2). The cohesive energies (E_{coh}) (binding or formation energies) could be calculated using the following formula, as implemented in GAUSSIAN 09 package [25,26].

$$E_{cho} = \frac{E_{tot} - \sum_i n_i E_i}{j}$$

where E_{tot}, E_i and n_i are the total energies of the drug-C₆₀ complexes, the atomic energy, and the amount of atoms type *i* (*i* = H, C, O, N, Cl, Si, B and Al), respectively, and *j* is the total number of atoms present in the drug-C₆₀ complexes.

In order to evaluate the nanocarrier, drug and complex reactivity, quantum descriptors such as global hardness (η), chemical potential (μ), electrophilicity index (ω), maximum charge transfer (ΔN_{max}), electronegativity (χ) and Fermi level (E_{FL}) were calculated. These indexes were estimated

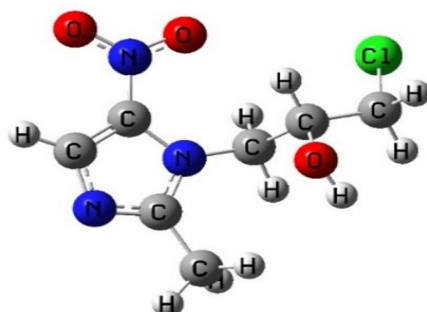


Fig. 1. Optimized structure of ornidazole (Orn.) drug.

through the following equations:

$$E_g = E_{LUMO} - E_{HOMO} \quad (2)$$

$$\mu = -\frac{IP + EA}{2} \quad (3)$$

$$\eta = \frac{E_{LUMO} - E_{HOMO}}{2} \quad (4)$$

$$\omega = \frac{\mu^2}{2\eta} \quad (5)$$

$$\Delta N_{\max} = -\frac{\mu}{\eta} \quad (6)$$

$$\chi = -\mu \quad (7)$$

$$E_{FL} = \frac{E_{LUMO} + E_{HOMO}}{2} \quad (8)$$

In these equations, E_{HOMO} and E_{LUMO} refer to the energies of HOMO and LUMO, respectively. IP and EA show the ionization and electron affinity energies. In addition, the thermodynamic parameters (ΔH_{ads} , ΔS_{ads} and ΔG_{ads}) were calculated to evaluate the drug adsorption possibility by the carriers [27].

RESULTS AND DISCUSSIONS

Molecular Electrostatic Potential (ESP)

At first, electrostatic potentials map (ESP) on the molecular surfaces of a single Orn. was computed, Fig. 2.

Since, red and blue colors in the ESP map show more negative and positive regions, respectively [28]. We can conclude that N and O atoms of the drug molecules shown in red color might be considered as the possible active site for the interaction with the fullerene and doped fullerenes. However, we investigated the interaction of the drug from a C site with fullerene and its derivatives. According to the electrostatic potentials map of C_{60} and the doped C_{60} fullerene, shown in Fig. 2, the active sites for $C_{59}B$, $C_{59}Al$ and $C_{59}Si$ are B, Al and Si atoms, respectively.

Optimization, Thermodynamic and Electronic Properties of the Structures

Configuration optimization all structures are performed using Gaussian 09 in theoretical level B3LYP/6-31G*. For doing so, the quantum mechanics calculations were carried out to elucidate the adsorption behavior of ornidazole drug on the surface of pristine as well as doped C_{60} fullerene with Si, B and Al (Fig. 3). All of these molecules were evaluated in this work.

In the next step, the bond lengths between drug and nanocarriers were calculated from optimized structures. The results suggested that the bond length for Orn.- C_{60} is lower than that for Orn.-cages (Table 1). $C_{59}Al$ -C-Orn. shows the greatest amounts for bond length. Discrepancy of bond length between doped cage-M-X-Orn. (M = B, Si, Al, X = C, N, O) can be attributed to the electronegativity difference of M and X atoms. For example, the bond lengths of cage-M-O-Orn. are 1.461, 1.661 and 1.745 Å for $C_{59}B$ -O-Orn, $C_{59}Si$ -O-Orn. and $C_{59}Al$ -O-Orn., respectively, (Fig. 4) that it is compatible to the electronegativity difference of M-O bond with values 1.461, 1.661 and 1.745

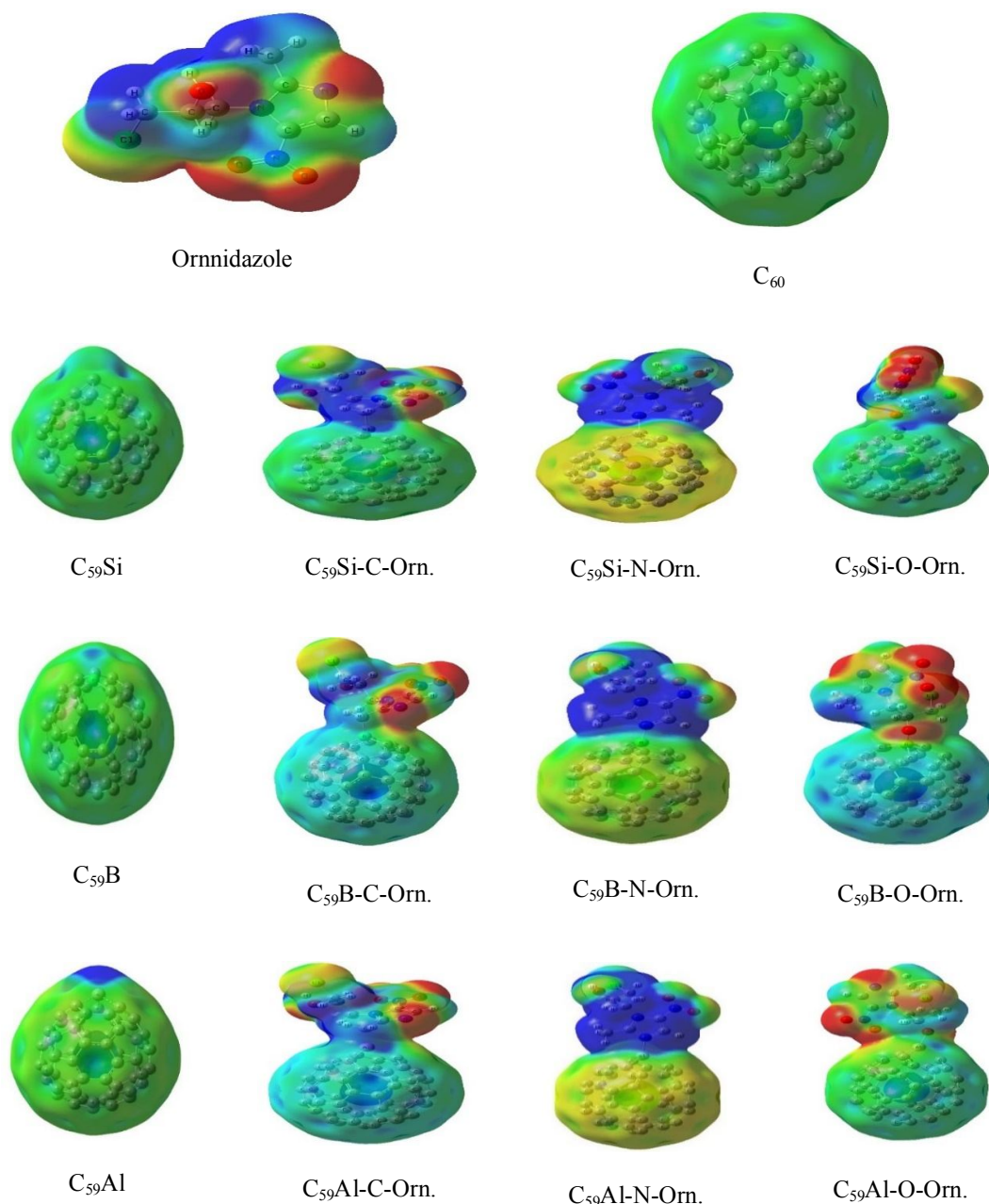


Fig. 2. The MEP images of drugs and drug-nanocarriers.

for B-O, Si-O and Al-O bonds.

Dipole moment (μ) expresses the amount of charge distribution and polarity in the molecule. The results show (Table 1) that the dipole moment of nano-cages in water is higher than that in the gas phase. Since water is the main part of the body, these conclusions suggest that the doping

may modify fullerenes drug delivery. As presented in Table 1, C_{60} has a zero value of dipole moment suggesting it is a non-polar molecule and the Orn. drug presents a dipole moment value of 6.12 Debye in gas phase and 6.26 Debye in water. Doping of the fullerene with the Si, B and Al atoms leads to a significant change in the dipole moment

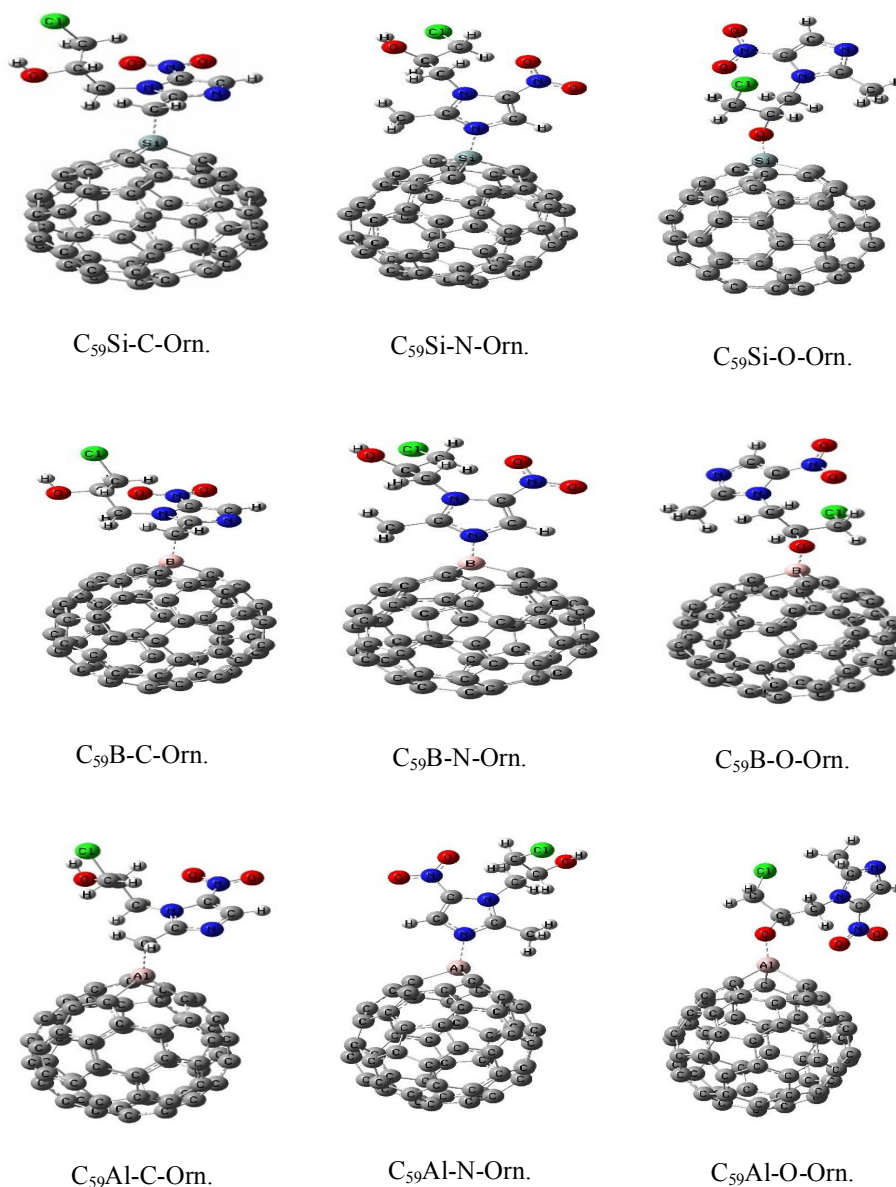


Fig. 3. Optimized structure of cage-M-X-Orn. (M = B, Si and Al, X = C, N and O).

especially in water. These values for $C_{59}M-N-Orn.$ (M = B, Al, Si) nanocages are higher than those for other complexes. The $C_{59}Si-N-Orn.$ nanocage shows a maximum dipole moment in water phase.

The stability of the drug-nanocarriers was evaluated by calculating the adsorption energy (Table 2). Based on the results, adsorption energies is negative for all nanocages except $C_{59}B-C-Orn.$, while these values for undoped- C_{60} are

positive. The E_b energies in solvent phase are high compared to the gaseous phase indicating more weakly interacted complexes in water solvent, except $C_{59}Si-N-Orn.$ that shows the highest E_b among nanocarriers in water phase with the value of $-655.47 \text{ kcal mol}^{-1}$. Finally, negative adsorption energy of drug-doped nanocages led to increasing in their stability. The negative value of binding energies (E_b) for $C_{59}Si-N-Orn.$ complex indicate that the

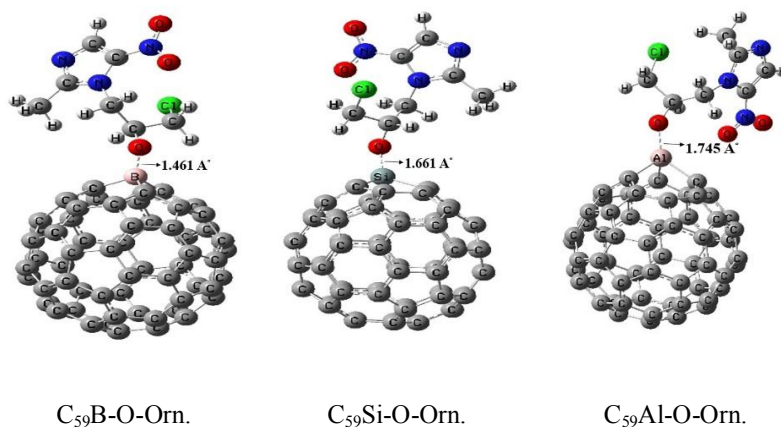


Fig. 4. Bond lengths (in Å) of cage-M-O-Orn. (M = B, Si and Al) complexes.

Table 1. Interatomic Distance of Drug-complex (in Å) and Dipole Moment (in D)

	Gas phase		Water phase	
	R	μ	R	μ
Ornidazole	-	6.12	-	6.26
C_{60}	-	0.00	-	0.00
$C_{59}Si$	-	0.28	-	0.52
$C_{59}Si-C-Orn.$	1.908	3.49	1.934	5.29
$C_{59}Si-N-Orn.$	1.911	13.11	1.905	18.08
$C_{59}Si-O-Orn.$	1.661	5.69	1.730	8.70
$C_{59}B$	-	0.48	-	0.94
$C_{59}B-C-Orn.$	1.683	7.47	1.690	10.96
$C_{59}B-N-Orn.$	1.630	8.53	1.612	11.11
$C_{59}B-O-Orn.$	1.461	10.96	1.503	15.29
$C_{59}Al$	-	2.88	-	5.21
$C_{59}Al-C-Orn.$	2.014	8.18	2.031	12.02
$C_{59}Al-N-Orn.$	1.995	12.18	1.965	15.97
$C_{59}Al-O-Orn.$	1.745	5.42	1.774	9.64

adsorbate drug shows an exothermic interaction with doped fullerene. The most negative binding energy among different configurations of this drug and pristine C_{60} is

observed for complex $C_{59}Si-X$ ($X = C, N, O$)-Orn in gas phase, indicating that this complex is the most stable structure among the other complexes. The ranges of

Table 2. Absorption Energies and Thermochemical Parameters for Drug-nanocages (kcal mol⁻¹)

		E_{coh}	E_{ad}	ΔH_{ad}	ΔG_{ad}	ΔS_{ad}
C ₅₉ Si-C-Orn.	Gas phase	-179.77	-29.89	-30.48	-19.10	-0.038
	Water phase	-171.48	352.72	352.12	363.46	0.038
C ₅₉ Si-N-Orn.	Gas phase	-178.32	-400.42	-425.00	-390.02	-0.117
	Water phase	-170.24	-655.47	-28.55	-16.48	0.041
C ₅₉ Si-O-Orn.	Gas phase	-174.20	-54.72	-55.32	-41.95	-0.045
	Water phase	-165.91	336.27	335.68	347.92	0.041
C ₅₉ B-C-Orn.	Gas phase	-179.95	4.73	4.14	16.80	-0.042
	Water phase	-171.95	368.51	367.91	325.77	-0.141
C ₅₉ B-N-Orn.	Gas phase	-178.74	-386.56	-387.16	-375.65	-0.039
	Water phase	-170.84	-29.24	-29.83	-73.46	-0.146
C ₅₉ B-O-Orn.	Gas phase	-174.25	-9.56	-10.15	2.04	-0.041
	Water phase	-166.35	354.62	354.03	311.07	-0.144
C ₅₉ Al-C-Orn.	Gas phase	-178.77	-17.68	-18.27	-6.89	-0.038
	Water phase	-170.68	354.63	354.03	366.73	0.043
C ₅₉ Al-N-Orn.	Gas phase	-177.59	-410.29	-410.88	-400.19	-0.036
	Water phase	-169.71	-47.55	-48.14	-33.88	0.048
C ₅₉ Al-O-Orn.	Gas phase	-173.28	-48.19	-49.56	-37.47	-0.041
	Water phase	-165.25	327.06	326.46	339.27	0.043

physisorption and chemisorption binding energies reported are 1-2 kcal mol⁻¹ and 10-100 kcal mol⁻¹, correspondingly [29]. The interaction mechanism of C₅₉B-X-Orn. (X = O, C) in gas phase is closer to physisorption range. The dominant interaction mechanism for other complexes in gas phase can be considered as chemisorption.

Thermodynamic parameters were calculated to investigate the drug adsorption possibility by the nanocarriers (Table 2). In gas phase, all of Gibbs energies values are negative except for the C₆₀-O-Orn. and

C₅₉B-C-Orn. systems. This confirms that adsorption of Orn. on the Si-, B- and Al-nanocarriers is spontaneous. The C₅₉Al-N-Orn. system showed the highest Gibbs energy. Therefore, doping caused to enhance the adsorption performance. Adsorption enthalpy values are negative in all cases except for the C₆₀-N-Orn. and C₅₉B-C-Orn. systems. This illustrates that the drug adsorption process is exothermic. The C₅₉Al-N-Orn. system presented the highest enthalpy (-100.33 kcal mol⁻¹). In all systems, adsorption entropy is negative, indicating that drug adsorption process

is accompanied by a disorder reduction that is reflected in adsorption mechanism. In water phase, only $C_{59}M-N-Orn.$ ($M = B, O, N$) complexes are spontaneous and have negative Gibbs energy. This results show drug adsorption process of these complexes in water phase is exothermic.

The images of HOMO and LUMO orbitals of the drug, pure and doped C_{60} and drug-doped complexes showed that these orbitals are located on the ring and the NO_2 groups (S-1). In addition, the frontier molecular orbitals of the C_{60} fullerene are almost symmetric. In the doped fullerenes, density of orbitals on the doped atom is higher than that on the other ones (specially for the Al-nanocages). LUMO orbitals in $C_{59}Si-N-Orn.$, $C_{59}B-N-Orn.$, $C_{59}Al-N-Orn.$ systems are located on the drug without any contribution of fullerene cages. E_g is a quantity that determines the reactivity of a molecule. According to Table 3, E_g of C_{60} is higher (2.87 eV) than that of doped- C_{60} : $C_{59}Si$, $C_{59}B$ and $C_{59}Al$ with values 2.24, 2.54 and 2.22 eV, respectively, leading to a higher tendency for doped molecules to the chemical interaction with Orn. On the other hand, E_g of Orn. is equal to 4.63 eV. E_g of drug-nanocages is lower than that of pure C_{60} and Orn. Table 2 also presents the values of E_g for N-nanocages: $C_{59}Si-N-Orn.$, $C_{59}B-N-Orn.$ and $C_{59}Al-N-Orn.$ (0.69, 1.31 and 0.91 eV) that are much lower than those for other systems ($\approx 1.6-2.3$ eV). Fermi levels (E_{FL}) of Orn., fullerene, and nanocages are in agreement with the E_g values. Fermi level is the highest energy state occupied by electrons in a material at absolute zero temperature. To better understand the electronic changes of the evaluated systems after drug absorption, density of states (DOS) were calculated (Fig. 5).

Physically, chemical potential (μ) describes the tendency of an electron to escape an equilibrium system. Negative values of chemical potential show that charge transfer between two particles is easy. The charge is transferred from a particle with a higher chemical potential to a particle with a lower chemical potential. In present work, the chemical potential electron (μ) for all drug-cages is negative in the range of -4.23 to -5.34 eV in gas and water phases. Table 3 shows that the chemical potential of Orn. is higher than nano hetrofullerenes $C_{59}M$ ($M = B, Al, Si$) in water phase. This means that electrons are transferred from the drug to the nanofullerenes. Therefore, the drug is well absorbed by the nano carrier.

In a molecule, chemical hardness expresses resistance to changes in electron distribution or electron transfer or charge transfer. There is a direct relationship between chemical hardness and energy gap. Higher chemical hardness and energy gap means the reduced reactivity. The chemical hardness of fullerene reduced after doping and also absorption of drug by C_{60} toward the N-site of drug. Table 3 shows that chemical hardness for N-nanocages: $C_{59}M-N-Orn$ ($M = B, Al, Si$) has the lowest values in gas and water phases.

In organic chemistry, electrophiles have empty orbitals for electron absorption. When two particles react together, one acts as an electrophile and the other as a nucleophile. Electrophilicity (ω) is a parameter related to chemical potential and chemical hardness. In this research, ω for all of the molecules is high. Also, this parameter for nanocages-N-Orn. is higher than that for other cages. Overall, chemical hardness values of complexes increase from gaseous to water media, whereas electrophilicity indexes of these structures decrease in water media.

Maximum charge transfer (ΔN_{max}) shows the charge capacity of the particle. According to the ΔN_{max} equation (Eq. (6)), when the chemical potential increases, the chemical hardness decreases and the electrophilicity increases. The results showed that (Table 3) the level of this parameter in N-nanocages-Orn is higher than that in other molecules. Based on the results, attachment of Orn. to nanofullerene from N-site has higher values in electrophilicity and electrical charge rather than C- and O-sites. Values of ΔN_{max} decrease from gaseous to water phase.

Ornidazol Drug Release

We know that the pH of target cells is lower than that of healthy cells [30-32]. Therefore, when the drug nano carrier reaches the target cell, it can be protonated from different sites. The presence of N and O in the structure of ornidazole drug increases the ability of nano fullerene as a drug carrier, because the ability of N and O atoms to protonation in acidic environment weakens their binding to fullerene in the target cell. For example, protonation of O atom in $C_{59}Al-O-Orn.$ ($HC_{59}Al-O-Orn.$) increased Al-O bond from 1.745 to 2.04 Å (Fig. 6). Therefore, in the target cell the drug easily leaves the fullerene. Therefore, the study of the

Table 3. Molecular Orbital Energies and Quantum Descriptors (eV)

		E_{HOMO}	E_{LUMO}	E_g	μ	η	ω	ΔN_{max}	χ	EFL
Ornonidazole	Gas phase	-6.97	-2.34	4.63	-4.66	2.31	4.68	2.02	4.66	-4.66
	Water phase	-7.25	-3.12	4.13	-5.18	2.06	5.81	2.51	5.18	-5.18
C_{60}	Gas phase	-6.25	-3.38	2.87	-4.81	1.43	8.06	3.36	4.81	-4.81
	Water phase	-6.07	-3.20	2.87	-4.63	1.43	7.50	3.24	4.63	-4.63
$C_{59}\text{Si}$	Gas phase	-6.07	-3.83	2.25	-4.95	1.12	10.91	4.42	4.95	-4.95
	Water phase	-5.89	-3.65	2.24	-4.77	1.12	10.16	4.26	4.77	-4.77
$C_{59}\text{Si-C-Orn.}$	Gas phase	-5.54	-3.30	2.24	-4.42	1.12	8.72	3.95	4.42	-4.42
	Water phase	-5.45	-3.22	2.23	-4.33	1.11	8.45	3.90	4.33	-4.33
$C_{59}\text{Si-N-Orn.}$	Gas phase	-4.70	-4.01	0.69	-4.36	0.34	27.61	12.82	4.36	-4.36
	Water phase	-4.90	-3.81	1.09	-4.35	0.54	17.52	8.06	4.35	-4.35
$C_{59}\text{Si-O-Orn.}$	Gas phase	-5.66	-3.38	2.28	-4.52	1.14	8.96	3.96	4.52	-4.52
	Water phase	-5.57	-3.23	2.34	-4.40	1.17	8.27	3.76	4.40	-4.40
$C_{59}\text{B}$	Gas phase	-5.91	-3.37	2.54	-4.64	1.27	8.47	3.65	4.64	-4.64
	Water phase	-5.74	-3.20	2.54	-4.47	1.27	7.87	3.52	4.47	-4.47
$C_{59}\text{B-C-Orn.}$	Gas phase	-6.13	-4.24	1.89	-5.18	0.95	14.20	5.45	5.18	-5.18
	Water phase	-6.02	-4.08	1.94	-5.05	0.97	13.15	5.21	5.05	-5.05
$C_{59}\text{B-N-Orn.}$	Gas phase	-4.88	-3.57	1.31	-4.23	0.65	13.68	6.51	4.23	-4.23
	Water phase	-5.04	-3.61	1.43	-4.32	0.71	13.14	6.08	4.32	-4.32
$C_{59}\text{B-O-Orn.}$	Gas phase	-6.24	-4.45	1.79	-5.34	0.90	15.94	5.93	5.34	-5.34
	Water phase	-6.06	-4.25	1.81	-5.15	0.90	14.73	5.72	5.15	-5.15
$C_{59}\text{Al}$	Gas phase	-5.60	-3.38	2.23	-4.49	1.11	9.05	4.05	4.49	-4.49
	Water phase	-5.42	-3.11	2.31	-4.26	1.15	7.89	3.70	4.26	-4.26
$C_{59}\text{Al-C-Orn.}$	Gas phase	-6.03	-4.43	1.61	-5.23	0.80	17.04	6.54	5.23	-5.23
	Water phase	-5.91	-4.24	1.67	-5.07	0.83	15.48	6.11	5.07	-5.07
$C_{59}\text{Al-N-Orn.}$	Gas phase	-4.79	-3.87	0.91	-4.33	0.46	20.57	9.41	4.33	-4.33
	Water phase	-5.04	-3.71	1.33	-4.37	0.66	14.47	6.62	4.37	-4.37
$C_{59}\text{Al-O-Orn.}$	Gas phase	-5.88	-4.29	1.59	-5.08	0.79	16.25	6.43	5.08	-5.08
	Water phase	-5.91	-4.27	1.64	-5.09	0.82	15.80	6.21	5.09	-5.09

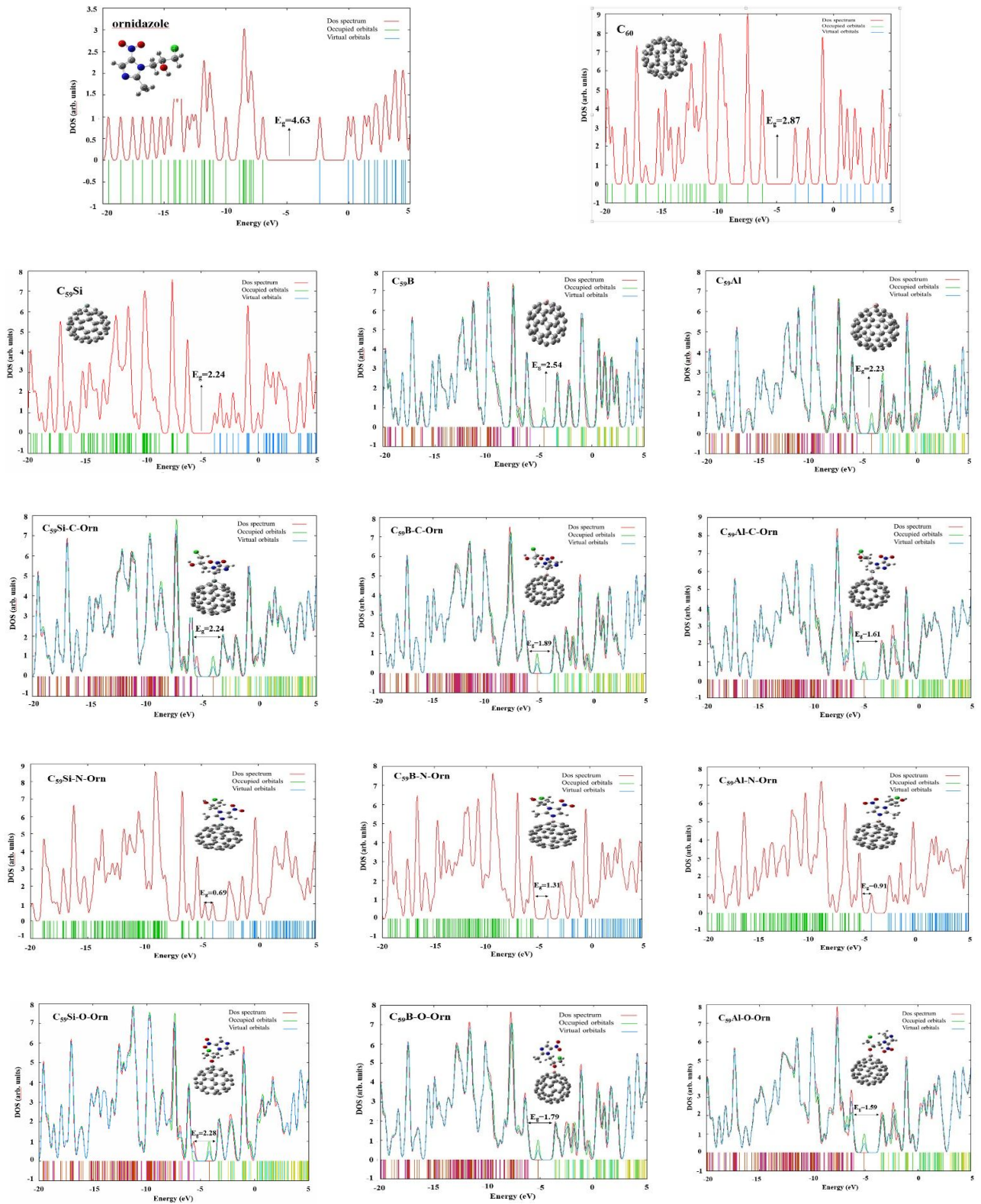


Fig. 5. Schematic of optimized structures and DOS plots for drugs and drug-nanocarriers.

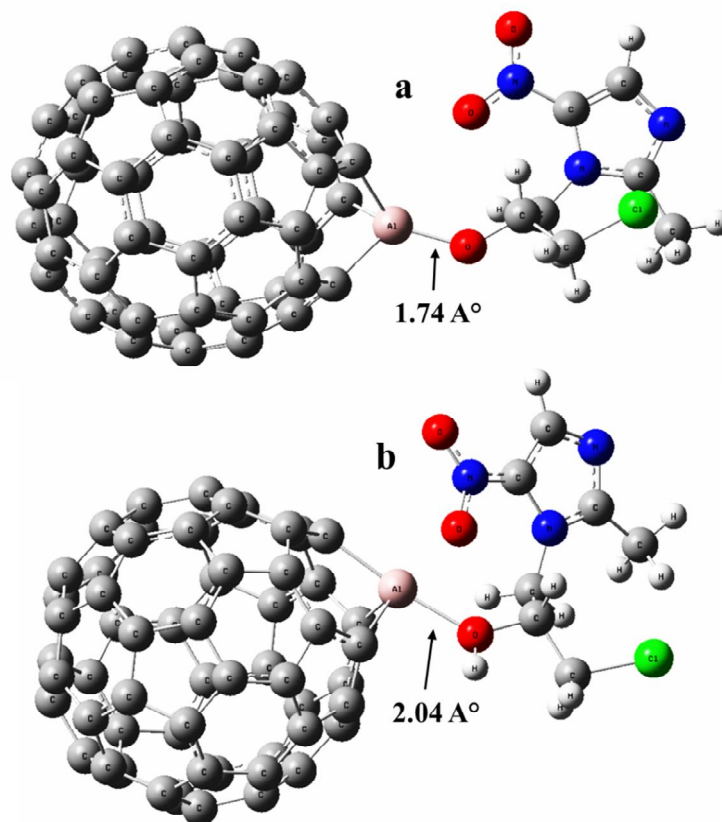


Fig. 6. Structure of a) $C_{59}Al-O-Orn$, and b) $HC_{59}Al-O-Orn$. fullerene.

drug release mechanism shows that with increasing the bond length $M-X$ ($X = O, N$ and $M = B, Al, Si$) in studied nano fullerenes, the tendency of the drug to release in the target cells increases. In this way, we can use these systems as candidates for drug delivery.

CONCLUSIONS

In this study, DFT calculations were performed to study the interactions between pristine C_{60} fullerene and also the B, Al, Si doped fullerene with ornidazole drug in order to investigate these compounds in drug design for treatment of amoebas and unicellular. Some important parameters were calculated and reported in this work. The ESP images displayed that the regions containing O and N in the ornidazole drug have the affinity to the nucleophile role in the reaction. The negative adsorption energies of drug-doped nanocages led to increasing in their stability. The

most negative binding energy among different configurations of this drug and pristine C_{60} is observed for complexes $C_{59}Si-X$ ($X = C, N, O$)-Orn., indicating that these complexes are generally the most stable structures among the other complexes in gas phase and $C_{59}Si-N-Orn.$ is the most stable among other complexes in water phase. On the other hand, the highest adsorption energy is shown in the $C_{59}Al-N-Orn.$ system ($-102.92 \text{ kcal mol}^{-1}$). It can be concluded that the weak interaction of C_{60} and drug was altered to strong chemisorption by interaction fullerene and N-site drug in gas phase. Also, the results confirm that adsorption of Orn. on the Si-, B- and Al-nanocarriers are spontaneous. The $C_{59}Al-N-Orn$ system showed the highest Gibbs free energy in gas phase but only $C_{59}M-N-Orn.$ ($M = B, O, N$) complexes are spontaneous and have negative Gibbs free energy in water phase.

The E_g of drug-nanocages is lower than that of pure C_{60} and Orn. Also, the values of E_g for N-nanocages:

C₅₉Si-N-Orn., C₅₉B-N-Orn, and C₅₉Al-N-Orn (0.69, 1.31 and 0.91 eV) are much lower than other systems (≈ 1.6 -2.3 eV). Chemical potential electron (μ) for all drug-cages are negative in the range of -4.23 to -5.34 eV. Chemical hardness has reduced after drug adsorption by doped-C₆₀ from the N-site of drug. Parameter ω for all of the molecules is high (≈ 8.5 -27.6 eV). Also, this parameter for nanocages-N-Orn is higher than that for other cages (≈ 13.7 -27.6 eV).

The decrease in E_g of C₆₀ as a result of interaction with drug in configuration N-site is smaller than that of the other configurations of this drug. So, these complexes are an electronically harmless interaction and the nano vehicle would not significantly alter the drug properties. Increases of electrophilicity index of nanocages-N-Orn relative to the single drug and C₆₀ means that the interaction of drug with fullerene has produced more electrophilic characteristic for the examined structures.

On the basis of all the obtained results, we can conclude that the doped C₆₀ fullerene, particularly C₅₉Al-N-Orn. and C₅₉Si-N-Orn., could be the better nano carriers for ornidazole drug delivery or nano sensor compared to the pristine C₆₀ fullerene due to their better reactivity, better electronic and magnetic properties and the more favorable thermodynamic properties.

REFERENCES

- [1] Schwartz, D. E.; Jeunet, F., Comparative pharmacokinetic studies of ornidazole and metronidazole in man. *Chemotherapy*, **1976**, *22*, 19-29, DOI: 10.1159/000221906.
- [2] Faramarzi, R.; Falahati, M.; Mirzaei, M., Interactions of fluorouracil by CNT and BNNT: DFT analyses. *Adv. J. Sci. Eng.* **2020**, *30*, 62-66, DOI: <https://doi.org/10.22034/AJSE.2012062>.
- [3] Mirzaei, M.; Gülseren, O.; Hadipour, N., DFT explorations of quadrupole coupling constants for planar 5-fluorouracil pairs. *Comput. Theor. Chem.* **2016**, *15*, 67-73, DOI: <https://doi.org/10.1016/j.comptc.2016.06.004>.
- [4] Kouchaki, A.; Gülseren, O.; Hadipour, N.; Mirzaei, M., Relaxations of fluorouracil tautomers by decorations of fullerene-like SiCs: DFT studies. *Phys. Lett. A.* **2016**, *380*, 2160-2166, DOI: <https://doi.org/10.1016/j.physleta.2016.04.037>.
- [5] Harismah, K.; Sadeghi, M.; Baniasadi, R.; Mirzaei, M., Adsorption of vitamin C on a fullerene surface: DFT studies. *J. Nanoanalysis.* **2017**, *4*, 1-7, DOI: 10.22034/jna.2017.01.001.
- [6] Zhao, L.; Li, H.; Tan, L., A novel fullerene-based drug delivery system delivering doxorubicin for potential lung cancer therapy. *J. Nanosci. Nanotechnol.* **2017**, *17*, 5147-5154, DOI: 10.1166/jnn.2017.13789.
- [7] Zhang, Q.; Wu, Z.; Li, N.; Pu, Y.; Wang, B.; Zhang, T.; Tao, J., Advanced review of graphene-based nanomaterials in drug delivery systems: Synthesis, modification, toxicity and application, *Mat. Sci. Eng. C-Mater.* **2017**, *77*, 1363-1375, DOI: 10.1016/j.msec.2017.03.196.
- [8] Illum, L.; Davis, S. S.; Wilson, C. G.; Tomas, N. W.; Frier, M.; Hardi, J. G., Blood clearance and organ deposition of intravenously administered colloidal particles-the effects of particle-size, nature and shape, *Int. J. Pharm.* **1982**, *12*, 135-146. DOI: [org/10.1016/0378-5173\(82\)90113-2](https://doi.org/10.1016/0378-5173(82)90113-2).
- [9] Ferrari, M., Cancer nanotechnology: Opportunities and challenges. *Nat. Rev. Cancer*, **2005**, *5*, 161-171. DOI: 10.1038/nrc1566.
- [10] Geng, Y.; Dalhaimer, P.; Cai, S.; Tesi, R.; Tewari, M.; Minko, T.; Discher, D. E., Shape effects of filaments versus spherical particles in flow and drug delivery. *Nat. Nanotechnol.* **2007**, *2*, 249-55. DOI: 10.1038/nnano.2007.70.
- [11] Kamel, M.; Raissi, H.; Morsali, A.; Shahabi, M., Assessment of the adsorption mechanism of Flutamide anticancer drug on the functionalized single-walled carbon nanotube surface as a drug delivery vehicle: An alternative theoretical approach based on DFT and MD. *Appl. Surf. Sci.* **2018**, *434*, 492-503, DOI: 10.1016/j.apsusc.2017.10.165.
- [12] Hasanzade, Z.; Raissi, H., Density functional theory calculations and molecular dynamics simulations of the adsorption of ellipticine anticancer drug on graphene oxide surface in aqueous medium as well as under controlled pH conditions. *J. Mol. Liq.* **2018**, *255*, 269-278, DOI: 10.1016/j.molliq.2018.01.159.

- [13] Shaffei, F.; Hashemianzadeh, S. M.; Bagheri, Y., Insight into the encapsulation of gemcitabine into boron-nitride nanotubes and gold cluster triggered release: A molecular dynamics simulation. *J. Mol. Liq.* **2019**, *278*, 201-212, DOI: 10.1016/j.molliq.2019.01.020.
- [14] Khodam Hazrati, M.; Hadipour, N., Adsorption behavior of 5-fluorouracil on pristine, B-, Si- and Al-doped C60 fullerenes: A first-principles study, *Phys. Lett. A* **2016**, *380*, 937-941. DOI: 10.1016/j.physleta.2016.01.020
- [15] M. R. Aram Bagheri Novir, S.; Quantum mechanical simulation of Chloroquine drug interaction with C60 fullerene for treatment of COVID-19. *Chem. Phys. Lett.* **2020**, *757*, 137869. DOI: 10.1016/j.cplett.2020.137869.
- [16] Geng, D.; Yang, S.; Zhang, Y.; Yang, J.; Liu, J.; Li, R.; Sham, T. K.; Sun, X.; Ye, S.; Knights, S., Nitrogen doping effects on the structure of graphene. *Appl. Surf. Sci.* **2011**, *257*, 9193-9198, DOI: 10.1016/j.apsusc.2011.05.131.
- [17] Khodadadei, F.; Safarian, S.; Ghanbari, N., Methotrexate-loaded nitrogen-doped graphene quantum dots nanocarriers as an efficient anticancer drug delivery system. *Mat. Sci. Eng. C-Mater.* **2017**, *79*, 280-285, DOI: 10.1016/j.msec.2017.05.049.
- [18] Fekri, M. H.; Omrani, A.; Jamehbozorgi, S.; Razavi Mehr, M., Study of electrochemical and electronical properties on the some schiff base Ni complexes in DMSO solvent by computational methods, *Adv. J. Chem. A* **2019**, *2*, 14-20, DOI: 10.29088/sami/AJCA.2019.2.1420.
- [19] Naderi, E.; Mirzaei, M.; Saghaie, L.; Khodarahmi, Gh.; Gulseren, O., Relaxations of methylpyridineone tautomers at the C60 surfaces: DFT studies, *Int. J. Nano Dimens.* **2017**, *8*, 124-131, DOI: 10.22034/ijnd.2017.24878.
- [20] Hasan, M.; Kumer, A.; Chakma, U., Theoretical investigation of doping effect of Fe for SnWO₄ in electronic structure and optical properties: DFT based first principle study, *Adv. J. Chem. A* **2020**, *3*, 639-644, DOI: 10.33945/SAMI/AJCA.2020.5.8.
- [21] Nabati, M.; Bodaghi-Namileh, V., Evaluation of medicinal effects of isoxazole ring isosteres on zonisamide for autism treatment by binding to potassium voltage-gated channel subfamily D member 2 (Kv 4.2), *Adv. J. Chem. A* **2020**, *3*, 462-472, DOI: 10.33945/SAMI/AJCA.2020.4.8.
- [22] Nabati, M.; Bodaghi-Namileh, V., Molecular modeling of 3-(1,3-dioxisoindolin-2-yl) benzyl nitrate and its molecular docking study with phosphodiesterase-5 (PDE5), *Adv. J. Chem. A* **2020**, *3*, 58-69, DOI: 10.33945/SAMI/AJCA.2020.1.7.
- [23] Fekri, M. H.; Bazvand, R.; Solymani, M.; Razavi Mehr, M., Adsorption of metronidazole drug on the surface of nano fullerene C₆₀ doped with Si, B and Al: A DFT Study, *Int. J. Nano Dimens.*, **2020**, *11*, 346-354. DOI: 10.22034/ijnd.2020.1901462.1910.
- [24] Frisch, M. J.; Trucks, G. W.; Schlegel, H. B.; Scuseria, G. E.; Robb, M. A.; Cheeseman, J. R.; Scalmani, G.; Barone, V.; Mennucci, B.; Petersson, G. A.; Nakatsuji, H.; Caricato, M.; Li X.; Hratchian, H. P.; Izmaylov, A. F.; Bloino, J.; Zheng, G.; Sonnenberg, J. L.; Hada, M.; Ehara, M.; Toyota, K.; Fukuda, R.; Hasegawa, J.; Ishida, M.; Nakajima, T.; Honda, Y.; Kitao, O.; Nakai, H.; Vreven, T.; Montgomery, Jr. J. A.; Peralta, J. E.; Ogliaro, F.; Bearpark, M.; Heyd, J. J.; Brothers, E.; Kudin, K. N.; Staroverov, V. N.; Kobayashi, R.; Normand, J.; Raghavachari, K.; Rendell, A.; Burant, J. C.; Iyengar, S. S.; Tomasi, J.; Cossi, M.; Rega, N.; Millam, J. M.; Klene, M.; Knox, J. E.; Cross, J. B.; Bakken, V.; Adamo, C.; Jaramillo, J.; Gomperts, R.; Stratmann, R. E.; Yazyev, O.; Austin, A. J.; Cammi, R.; Pomelli, C.; Ochterski, J. W.; Martin, R. L.; Morokuma, K.; Zakrzewski, V. G.; Voth, G. A.; Salvador, P.; Dannenberg, J. J.; Dapprich, S.; Daniels, A. D.; Farkas, Ö.; Foresman, J. B.; Ortiz, J. V.; Cioslowski, J.; Fox, D. J., GAUSSIAN 09, Revision A.1, GAUSSIAN Inc., Wallingford, CT., 2009.
- [25] Zheng, Y.; Shan, K.; Zhang, Y.; Gu, W., Amino acid-functionalized borospherenes as drug delivery systems. *Biophys. Chem.*, **2020**, *263*, 106407-106423, DOI: 10.1016/j.bpc.2020.106407.
- [26] Siqui, J.; Shasha, Y.; Xiao, W.; Gu, W., T-graphene and its boron nitride analogue as versatile drug delivery systems. *Mol. Phys.*, **2020**, *118*, e1757775, DOI: 10.1080/00268976.2020.1757775.

- [27] Ghasemi, A. S.; Ramezani Taghartapeh, M.; Soltani, A.; Mahon, P. J., Adsorption behavior of metformin drug on boron nitride fullerenes: Thermodynamics and DFT studies. *J. Mol. Liq.* **2019**, *275*, 955-967, DOI: <https://doi.org/10.1016/j.molliq.2018.11.124>.
- [28] Parlak, C.; Alver, O.; A density functional theory investigation on amantadine drug interaction with pristine and B, Al, Si, Ga, Ge doped C60 fullerenes. *Chem. Phys. Lett.* **2017**, *678*, 85-90. DOI: [org/10.1016/j.cplett.2017.04.025](https://doi.org/10.1016/j.cplett.2017.04.025).
- [29] Bhushan, B.; Principles and Applications of Tribology. 1st ed. USA: Wiley-Interscience, **1999**, p. 95.
- [30] Hazrati, M. K.; Bagheri, Z.; Bodaghi, A., Application of C₃₀B₁₅N₁₅ heterofullerene in the isoniazid drug delivery: DFT studies, *Physica E*, **2017**, *89*, 72-76. DOI: [10.1016/j.physe.2017.02.009](https://doi.org/10.1016/j.physe.2017.02.009).
- [31] Nagarajan, V.; Chandiramouli, R., A study on quercetin and 5-fluorouracil drug interaction on graphyne nanosheets and solvent effects-A first-principles study, *J. Mol. Liq.* **2018**, *275*, 713-722 DOI: [10.1016/j.molliq.2018.11.083](https://doi.org/10.1016/j.molliq.2018.11.083).
- [32] U. Srimathi, U.; Nagarajan, V.; Chandiramouli, R., Interaction of imuran, pentasa and hyoscyamine drugs and solvent effects on graphdiyne nanotube as a drug delivery system-A DFT study, *J. Mol. Liq.* **2018**, *265*, 199-207. DOI:[10.1016/j.molliq.2018.05.114](https://doi.org/10.1016/j.molliq.2018.05.114).